BIOCHEMISTRY
including biophysical chemistry & molecular biology

Article

pubs.acs.org/biochemistry

Slow Folding and Assembly of a Procaspase-3 Interface Variant

Sarah H. MacKenzie and A. Clay Clark*

Department of Molecular and Structural Biochemistry, North Carolina State University, Raleigh, North Carolina 27695, United States

ABSTRACT: Caspases execute apoptosis and exist in the cell as inactive zymogens (procaspases) prior to activation. Initiator procaspases are monomers that must dimerize for activation, while effector procaspases, such as procaspase-3, are stable dimers that must be processed for activation. The dimer interface regions of the two subfamilies are different, although the role of the interface in oligomerization is not known. Equilibrium and kinetic folding studies were performed on procaspase-3(C163S,V266H), an interface variant, to determine the importance of the dimer interface in the folding of procaspase-3. Equilibrium folding data at pH 5 and 7 display a hysteresis, indicating a kinetically controlled folding reaction. Refolding kinetic studies reveal a complex burst phase, followed by a series of monomeric intermediates. At longer refolding times, the monomer populates a species that becomes kinetically trapped and slowly aggregates. Unfolding kinetic studies reveal a hyperfluorescent native ensemble that unfolds to form highly structured monomeric intermediates that unfold very slowly. Dimerization is very slow, likely because of the inability to correctly orient the histidine residues in the interface, so the initial encounter complex for dimerization is inefficient. As a consequence, the monomer folds into species that aggregate. Introducing a histidine into the interface of procaspase-3 prevents activation by acting as a negative design element, providing evidence that the interface region is a site of regulation of caspase assembly in general by affecting the rate of dimerization.

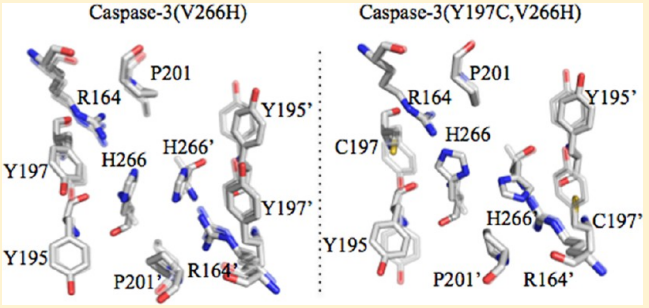

Caspases, a family of cysteine-dependent aspartate-directed proteases, are responsible for the cleavage of key proteins in the cell that lead to apoptosis. There are two groups of apoptotic caspases, the initiators and effectors, grouped as such by their time of entry into the apoptotic cascade.[1,2] Initiator caspases (-8, -9, and -10) make an early entry into the cascade and are responsible for activating the effector caspases (-3, -6, and -7). Once the effector caspases, specifically caspase-3, are activated, the cell is committed to undergo apoptosis. Both subfamilies are found in the cell as inactive zymogens (procaspases) that are rapidly converted to active proteases upon induction of apoptosis. Structural studies reveal a common fold, regardless of group or sequence identity, that contains a 12-stranded β-sheet core surrounded by a network of α-helices.[1,2] Procaspase-3 is a homodimer in which each monomer has 277 amino acids and is composed of an N-terminal prodomain, a large subunit, and a small subunit. The large and small subunits are covalently connected by an intersubunit linker (IL) that, once processed, contributes two (L2 and L2′) of the five active site loops (L1−L4), making dimerization a prerequisite for activation (Figure 1A).[3,4] An active caspase molecule is derived from the association and processing of two procaspase monomers. Processing of procaspase-3 occurs in an ordered manner, in which the IL is first cleaved at D175 and then the prodomain is removed following cleavages at D9 and D28.

A fundamental difference exists between the subfamilies regarding their oligomeric state prior to activation. Initiator procaspases are found in the cell as monomers that must dimerize for activation.[5−8] In this case, association occurs through recruitment to a multiprotein scaffold, which induces dimerization by increasing the local concentration of procaspase monomers at the onset of apoptosis. The IL is cleaved following dimerization, and while this stabilizes the dimer, cleavage of the linker is not necessary to realize an increase in enzymatic activity because a functional active site can form without this event. It has been stated that the fate of the cell depends on the oligomeric state of initiator procaspases because dimerization is the primary mechanism for regulating activity.[9] Conversely, effector procaspases are found in the cell as stable, inactive dimers that must be processed to increase enzymatic activity.[10−12] Activation of effector caspases occurs after proteolytic cleavage of the IL, resulting in the rearrangement of the active site loops. The difference in the oligomeric state of the two apoptotic caspase subfamilies prior to activation could be largely due to the composition of the amino acids in the dimer interface. The initiator procaspase-8, for example, contains negative design elements[13] in the interface that likely prevent indiscriminant associations of the exposed β-strand 8 in the monomer. No such elements are observed in the interfaces of effector procaspases. On the basis of the current understanding of procaspase association, it seems that understanding the interactions in the interface region is important in elucidating the differences in activation mechanisms, because the dimer interfaces of the two caspase subfamilies have significantly different properties and the

Received: January 30, 2013
Revised: April 24, 2013
Published: April 24, 2013

   dx.doi.org/10.1021/bi400115n | *Biochemistry* 2013, 52, 3415−3427

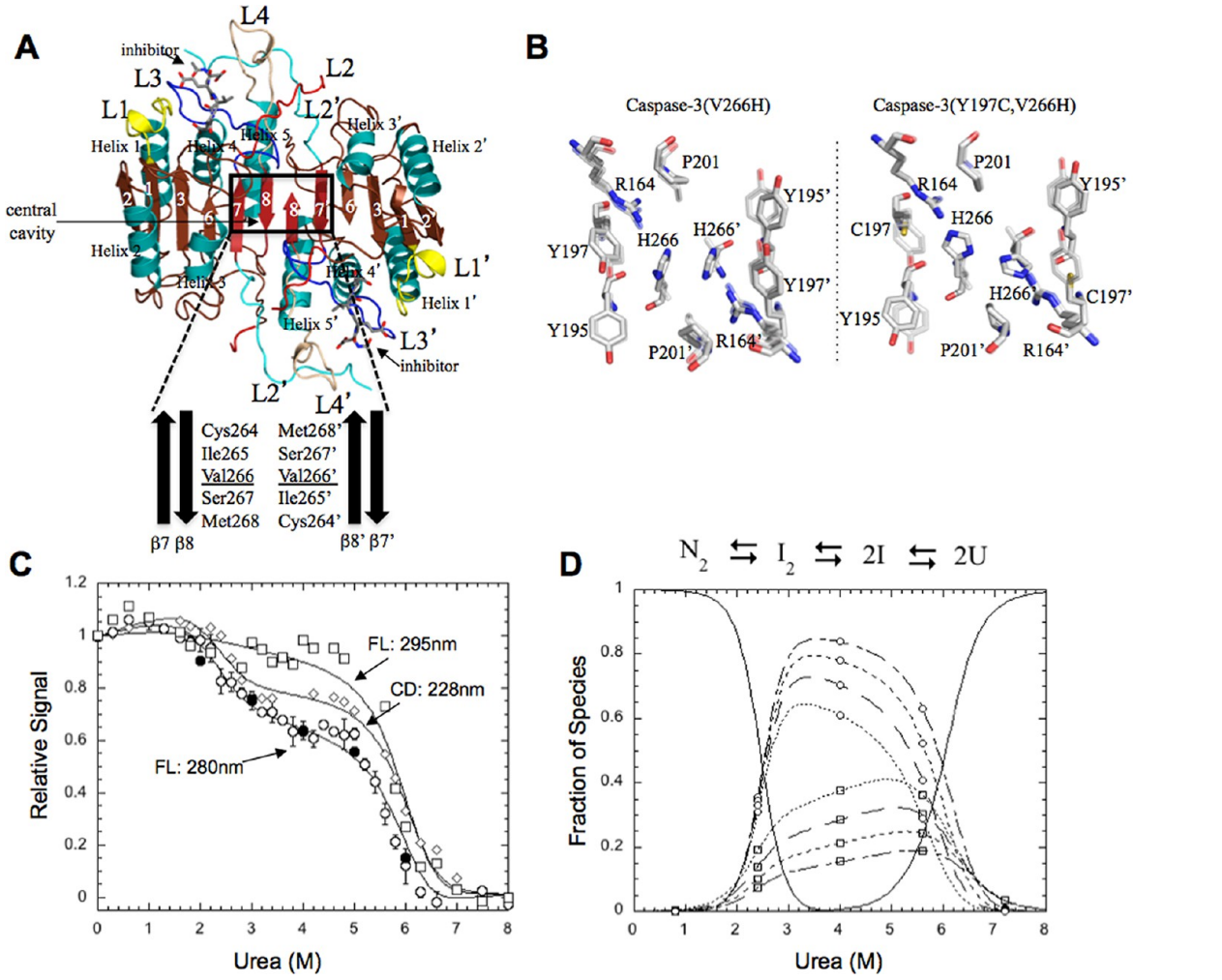

Figure 1. (A) Structure of caspase-3 highlighting the two active sites (L1−L4) and the dimer interface region (box) between the two small subunits. The residues listed under the structure are found in the dimer interface, highlighting the central valine at position 266. (B) Structure of the interface of procaspase-3(V266H) (left, PDB entry 4EHA) and procaspase-3(C197C,V266H) (right, PDB entry 4EHF). Replacement of Y197 with cysteine results in rotation of the H266 side chain to the more preferred rotamer because of the release of steric clashes in the interface. Both structures are overlaid with that of wild-type caspase-3 (PDB entry 2J30) (semitransparent). (C) Equilibrium unfolding of procaspase-3(C163S) ("wild type"). Unfolding was measured by CD at 228 nm (◇) and by fluorescence emission at 320 nm with excitation at either 280 (○) or 295 nm (□). Filled symbols (●) represent data for the refolded protein to show reversibility. (D) Fraction of species as a function of urea concentration. The fractions of native (N_2), dimeric intermediate (I_2), monomeric intermediate (I), and unfolded (U) protein were calculated at 0.25 (---), 0.5 (————), 1 (–––), and 2 μM (————) procaspase-3(C163S). Panels C and D were taken from ref 18. Copyright 2001 American Chemical Society.

initiator caspase zymogens do not require processing to gain activity.

To improve our understanding of the role of the interface in dimerization, we introduced a single-amino acid mutation, changing V266 to histidine, into the center of the dimer interface (Figure 1A,B). Previous data showed that the presence of H266 completely abolishes the activity of mature caspase-3 as well as that of procaspase-3.[14] More recently, structural and biochemical studies of caspase-3(V266H) revealed a disordered active site loop, L1, and a narrower substrate-binding pocket.[15] The mutation appears to destabilize helix 3 on the protein surface such that the helix transiently unfolds and rotates toward the dimer interface. Overall, when placed in the context of mature caspase-3, the V266 to His mutation shifts the native ensemble toward the inactive state, which is likely responsible for the loss of function.[15] Wells and co-workers showed that the binding of allosteric inhibitors in the interface prevents proper active site formation by blocking the movement of active site L3 into the interface, thus preventing formation of the substrate-binding pocket.[16,17] Our previous data for caspase-3(V266H) showed that, in addition to the large loop movements observed for the allosteric inhibitors, destabilizing the active ensemble also occurs via the destabilization of helix 3, even though the substrate-binding pocket is formed. Thus, allosteric inhibition involving the interface also involves more subtle structural changes that shift the ensemble of states toward the inactive conformer.

The focus of our research here is to investigate the importance of the dimer interface in the folding and assembly of procaspase-3 by elucidating the thermodynamic and kinetic folding mechanisms of procaspase-3(C163S,V266H). Equilibrium folding studies of wild-type procaspase-3 [that is, procaspase-3(C163S)] showed that the protein is very stable, with a conformational free energy of 25.8 kcal/mol at 25 °C.[18] The protein unfolds via a four-state equilibrium model, in which the native dimer isomerizes to a dimeric intermediate and the dimeric intermediate dissociates to a monomeric intermediate, which then unfolds (Figure 1C,D).[18] The data revealed that dimerization is a folding event because it occurs by the

dx.doi.org/10.1021/bi400115n | *Biochemistry* 2013, 52, 3415−3427

association of two partially folded monomeric species. In kinetic studies, we also showed that the procaspase-3 monomer folds through several intermediates, some of which appear to be off-pathway.[19] Assembly of the dimer is kinetically very slow, with a second-order rate constant for association of ~70 M^{-1} s^{-1}, suggesting the lack of stabilizing native interactions in the initial encounter complex. Modeling of procaspase-3(V266H) showed the potential for steric packing problems in the interface,[2] and the recently published structural data for mature caspase-3(V266H) support the model.[15]

The results presented here show that the equilibrium unfolding and refolding of the V266H variant display a hysteresis, indicating that a folding intermediate enters a kinetic trap in the energy landscape and does not reach the global minimum. We performed kinetic refolding and unfolding experiments to determine the effect of the mutation on folding, and the results show that at short times (<100 s) the mechanism is very similar to that of wild-type procaspase-3, determined previously.[19] At longer refolding times, however, the protein folds into a species that becomes kinetically trapped and is prone to aggregation. Unfolding kinetic studies reveal a hyperfluorescent native ensemble that first unfolds to a highly structured monomeric intermediate. The monomeric intermediate then unfolds very slowly. Together, the data suggest that very slow dimerization results in the formation of kinetically trapped and aggregation-prone species in the monomer, leading to hysteresis in the equilibrium folding−unfolding data.

MATERIALS AND METHODS

Materials. Ultrapure urea was purchased from ICN. Dithiothreitol (DTT), acrylamide, and imidazole were purchased from Acros. Sodium chloride (NaCl), trizma base (Tris), tryptone, and yeast extract were purchased from Fisher. Monobasic and dibasic potassium phosphate (KH_2PO_4 and K_2HPO_4, respectively), sodium citrate, citric acid, ampicillin, and molecular weight markers were purchased from Sigma. IPTG (isopropyl β-D-1-thiogalactopyranoside) was purchased from Anatrace. YM-10 membranes were purchased from Millipore. His-bind resin was purchased from Novagen. Q-Sepharose and molecular weight gel filtration calibration kits were purchased from Amersham Biosciences.

Stock Solutions. A urea stock solution (10 M) was prepared in 20 mM phosphate buffer (pH 6.5−7.0) or 20 mM sodium citrate buffer (pH 4.5−6.0) as described previously.[20,21] The molarity of the prepared urea was determined by molecular weight measurement and confirmed by the refractive index. Urea stock solutions were prepared fresh for each experiment and were filtered prior to use with a 0.45 μm filter.

Methods. *Protein Purification.* Procaspase-3(C163S) and procaspase-3(C163S,V266H) were purified as C-terminally His_6-tagged proteins from *Escherichia coli* BL21(DE3) LysS cells as previously described.[11,14] The concentrations of procaspase-3(C163S) and procaspase-3(C163S,V266H) were determined using an ε_{280} of 26500 M^{-1} cm^{-1}. It has been well established that at high procaspase-3 concentrations, such as those required for protein expression, there is a small amount of caspase-3 activation caused by autocatalysis.[22−25] To prevent autolysis, we replaced the catalytic cysteine with a serine residue (C163S). The introduction of serine into this position prevents autolysis and does not significantly alter the structure.[18,26,27] Here, procaspase-3(C163S) is termed the "wild-type" protein, and both equilibrium and kinetic folding studies utilizing this protein were described previously.[18,19]

Equilibrium Folding Studies. Equilibrium folding studies with the V266H variant were performed as described previously.[18,20] Briefly, 50 μM protein stock solutions were prepared in 20 mM phosphate buffer (pH 7.0) or 20 mM citrate buffer (pH 5.0). The unfolding samples were prepared from 0 to 9 M urea in 0.25 M increments and incubated for 24 h. The refolding samples were unfolded in 9 M urea for 24 h prior to the addition to various concentrations of urea-containing buffers in 1 M increments.

Fluorescence emission scans were measured using a PTI C-61 spectrofluorometer (Photon Technology International, Birmingham, NJ). Time-based measurements were acquired with excitation wavelengths of 280 and 295 nm with fluorescence emission at 340 nm. Circular dichroism was measured using a PiStar spectrophotometer (Applied Photophysics, Surrey, U.K.) at 228 nm. The data were averaged for 20 s using both detection methods. All measurements were corrected for the background signal. Both instruments were equipped with a water jacket to maintain a constant temperature of 25 °C.

A comparison of the fluorescence emission profiles of procaspase-3(C163S,V266H) and the wild type shows identical emission characteristics upon excitation at 280 or 295 nm, where the peak maxima occur at 335 and 340 nm, respectively.[18] Similarly, the CD spectra of both native proteins overlay with a negative ellipticity between 210 and 220 nm, indicative of a properly folded secondary structure.[11] Finally, a comparison of the elution profiles of native procaspase-3(C163S,V266H) and the wild type by size exclusion chromatography (SEC) shows identical elution volumes with a molecular mass of ~64 kDa (data not shown). These data, taken together, provide evidence that the V266H mutation in the dimer interface does not disrupt the global structure of the native protein.

Kinetic Folding Studies. All kinetic folding studies were performed as described previously,[19,28] with the following considerations.

Single-Mixing Stopped-Flow Fluorescence and CD. Single-mixing kinetic folding and unfolding experiments were performed using a stopped-flow spectrofluorometer (SX18) or spectrophotometer (PiStar) from Applied Photophysics. The temperature was controlled using a circulating water bath at 25 °C. Several techniques were used for single-mixing experiments and are described briefly. Fluorescence emission spectroscopy following excitation at 280 nm examines the tertiary structure of the protein by exciting both tyrosine and tryptophan residues. Procaspase-3(C163S,V266H) has two tryptophan residues per monomer, which are located in the active site, and 10 tyrosine residues per monomer, which are distributed throughout the polypeptide chain. Fluorescence emission spectroscopy following excitation at 295 nm examines the formation of the active site by selectively exciting only tryptophan residues. Far-UV circular dichroism (CD), measured at 228 nm, examines the secondary structure of the protein. Fluorescence anisotropy, with excitation at 280 or 295 nm, examines the rotation or tumbling of the protein. More nativelike ensembles will display a higher anisotropy value than unfolded or partially unfolded ensembles. Differential quenching by acrylamide, with excitation at 295 nm, provides additional information about the active site of the protein by observing the relative exposure of the tryptophan residues. In the cases of anisotropy and differential quenching studies following excitation at the wavelengths specified above, fluorescence emission was measured using a 305 nm cutoff filter.

Hand-Mixing Fluorescence and CD Spectroscopy. Hand-mixing folding studies were performed with a PTI C-61 spectrofluorometer (fluorescence emission and differential

dx.doi.org/10.1021/bi400115n | Biochemistry 2013, 52, 3415−3427

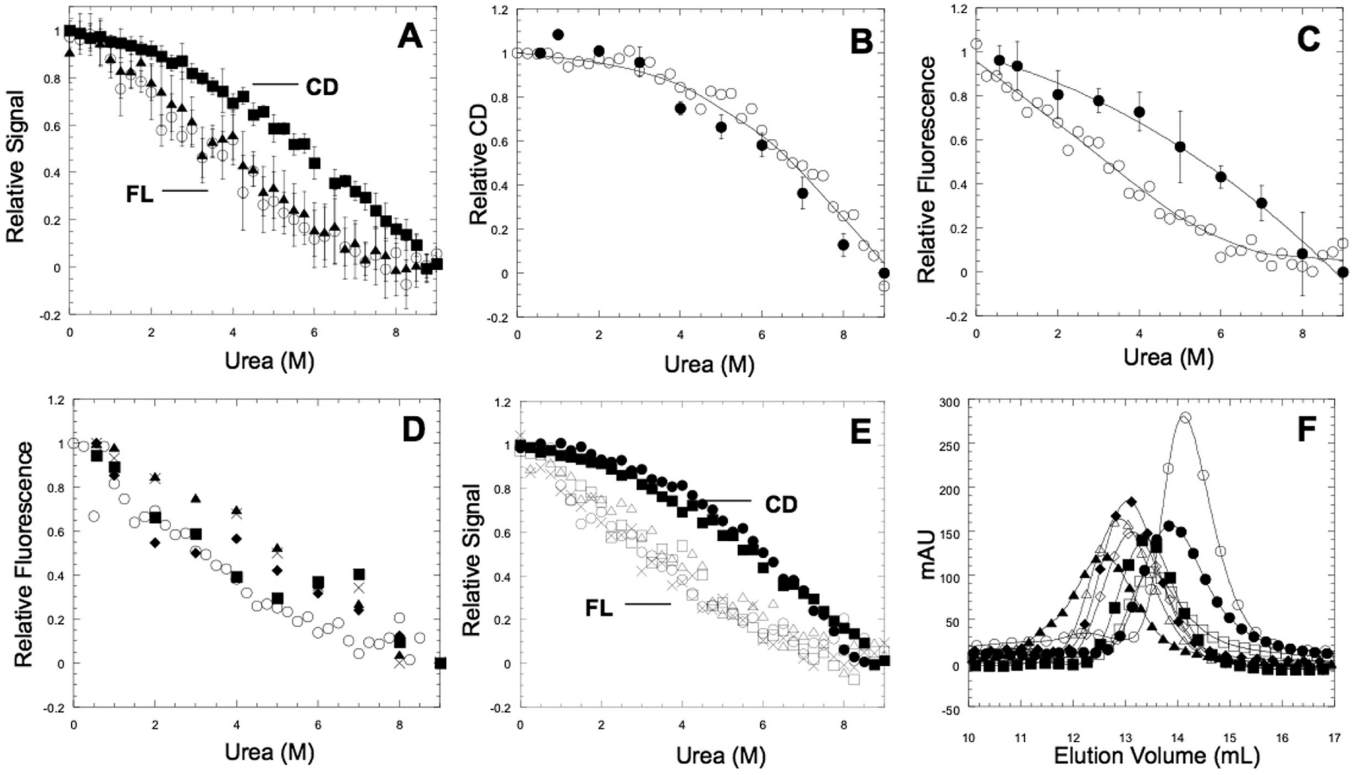

Figure 2. Equilibrium folding of procaspase-3(C163S,V266H) at pH 7.0. (A) Unfolding was measured by CD at 228 nm (■) and by fluorescence emission at 340 nm with excitation at either 280 (○) or 295 nm (▲) (representative protein concentration of 4 μM). Error bars represent the average from 10 experiments. (B and C) Reversibility. Unfolding (○) and refolding (●) were measured by CD at 228 nm (B) or by fluorescence emission at 340 nm with excitation at 295 nm (C) (representative protein concentration of 0.5 μM). Error bars for the refolding curves represent the average from five experiments. The lines through the data were added for the sake of clarity and do not represent fits. (D) Overlay of refolding curves that shows a concentration-dependent hysteresis. The unfolding curve for 2 μM protein (○) is plotted with the refolding curves for 4 (■), 2 (◆), 1 (×), and 0.5 μM protein (▲) excited at 280 nm. (E) Unfolding was measured by fluorescence emission at 340 nm with excitation at either 280 nm (FL) or by CD at 228 nm for the following protein concentrations and demonstrates no dependence on protein concentration: 4 (□ and ■), 2 (○ and ●), 1 (△), and 0.5 μM (×). (F) Denaturation profile determined by size exclusion chromatography. Overlaid chromatograms of protein at 0 (○), 1 (●), 2 (□), 3 (■), 4 (◇), 5 (◆), 6 (△), and 8 M urea (▲).

quenching by acrylamide experiments), a stopped-flow SX18 spectrofluorometer (anisotropy experiments), and a PiStar spectrophotometer (CD experiments) as described previously.[19] The dead time for mixing was ~20 s. The signal was monitored at the following wavelengths: 228 nm for CD, >305 nm for anisotropy and fluorescence emission (excitation at 280 nm), and 340 nm for differential quenching by acrylamide (excitation at 295 nm). The CD signal was monitored continuously over time, while the signals for both anisotropy and fluorescence measurements were monitored hourly.

Size Exclusion Chromatography (SEC). All sizing experiments were performed using a Superdex 200 10/300 GL sizing column on an AKTA FPLC system (Amersham Biosciences, Piscataway, NJ). SEC was used to determine the oligomeric properties of procaspase-3(C163S,V266H) at various urea concentrations, ranging from 0 to 8 M. Protein (1 mg/mL) was dialyzed overnight against at least 10 column volumes of the appropriate buffer.

For denaturation studies, procaspase-3(C163S,V266H) was dialyzed overnight against varying concentrations of urea-containing phosphate buffer (20 mM, pH 7) or urea-containing citrate buffer (20 mM, pH 5). After overnight dialysis, the protein was centrifuged to pellet any debris that could interfere with the column. Molecular weights were determined using elution profiles of known standards (HMW and LWM gel filtration calibration kits, Amersham Biosciences).

RESULTS

Equilibrium Folding of Procaspase-3(C163S,V266H) at pH 7 Is Not Reversible and Reveals a Protein Concentration-Dependent Hysteresis. The equilibrium folding transition of procaspase-3(C163S,V266H), unlike those of the wild type, displays a broad cooperative transition over a large range of urea concentrations [representative data at 2 μM (Figure 2A compared to Figure 1C)]. The $\text{urea}_{1/2}$ values for the transition are ~4 M for fluorescence emission (excited at 280 or 295 nm) and ~6 M when measured by CD, so the secondary structure remains intact over a larger range of urea concentrations than does the tertiary structure. The unfolding and refolding transitions are coincident when measured by CD at 228 nm at all protein concentrations (Figure 2B). In contrast, the data do not overlay when monitored by fluorescence emission (excited at 280 or 295 nm) (Figure 2C or not shown). The hysteresis occurs in a protein concentration-dependent manner, as the difference in the signal between the folding−unfolding curves decreases as the protein concentration increases (Figure 2D). For comparison, previous data for the equilibrium folding of procaspase-3(C163S) (here termed wild type) are shown in panels C and D of Figure 1, where the transitions are reversible at all protein concentrations tested.

We did not observe a protein concentration-dependent step during folding and unfolding by the techniques used in this study,

dx.doi.org/10.1021/bi400115n | *Biochemistry* 2013, 52, 3415−3427

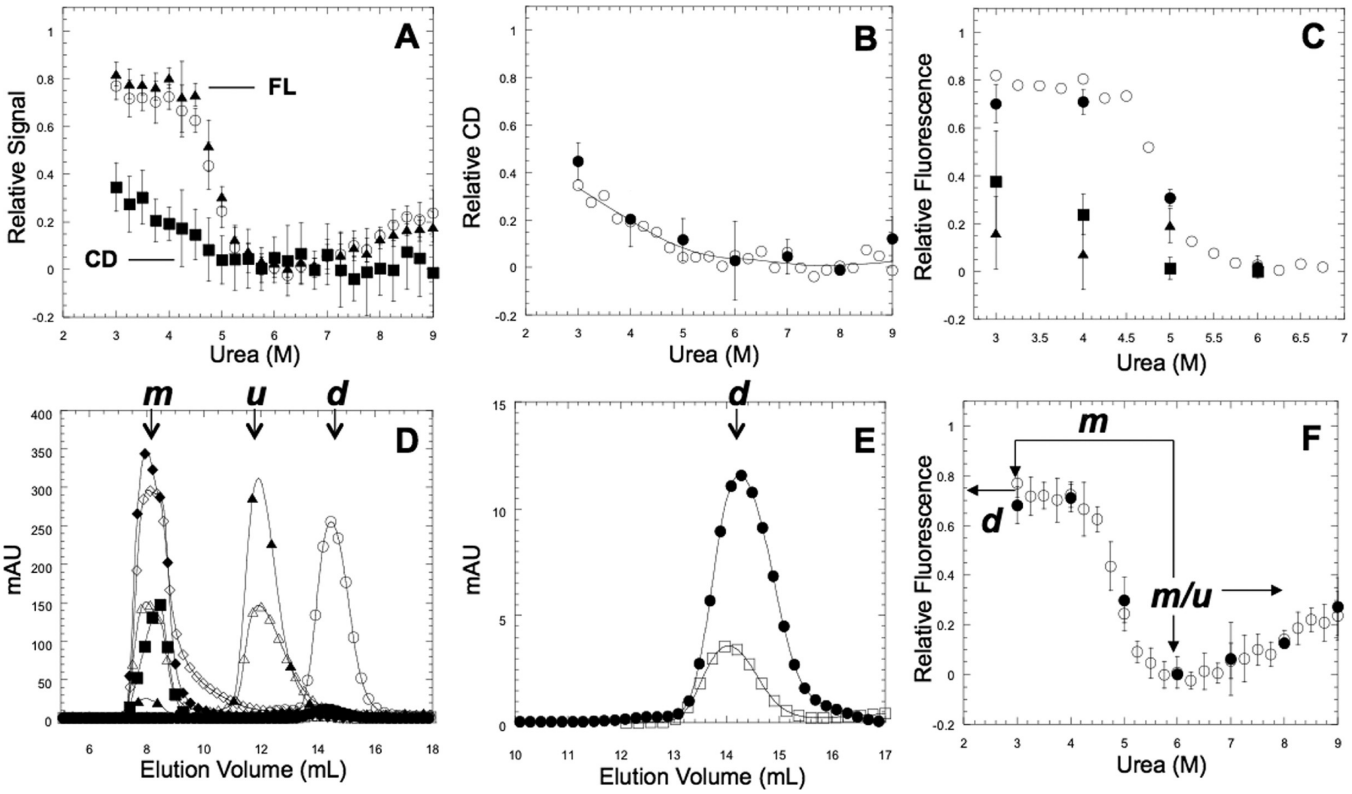

Figure 3. Equilibrium folding of procaspase-3(C163S,V266H) at pH 5.0. (A) Unfolding was measured by CD at 228 nm (■) and by fluorescence emission at 340 nm with excitation at either 280 (○) or 295 nm (▲) (representative protein concentration of 2 μM). Data are truncated because of precipitation during equilibration in samples between 0.25 and 3 M urea. Error bars represent the average from 10 experiments. (B and C) Reversibility. Unfolding at 2 μM protein (○) and refolding at 2 (●), 1 (■), and 0.5 μM protein (▲) were measured by CD at 228 nm (B) or by fluorescence emission at 340 nm with excitation at 295 nm (C). Error bars shown for the refolding curves represent the average of five experiments. The lines through the data were added for the sake of clarity and do not represent fits. (D and E) Denaturation profiles determined by size exclusion chromatography. Chromatograms of protein at 0 (○), 1 (●), 2 (□), 3 (■), 4 (◇), 5 (◆), 6 (△), and 8 M urea (▲). Labels above the plot represent monomer (m), unfolded protein (u), and dimer (d). (F) Sizing data reveal that the cooperative transition observed during unfolding is that of the monomer.

so it is unclear where dimerization occurs (Figure 2E). Consequently, we examined the oligomeric state of procaspase-3(C163S,V266H) at various urea concentrations by SEC (Figure 2F). The native dimer (○) has the largest elution volume, and we observed that the elution volume decreased as the concentration of urea increased, with the unfolded protein (▲) having the smallest elution volume. The data show that the shape of the protein changes as the concentration of urea increases such that the unfolded monomer is in an expanded conformation relative to the dimer. Because the monomer forms at high urea concentrations when it is unfolded at pH 7, the data suggest that the dimeric and monomeric species co-elute and cannot be separated at intermediate urea concentrations. On the basis of these data, we are unable to determine the range of urea concentrations at which the dimer dissociates into two monomers. Overall, the folding mechanism at pH 7 is substantially different for procaspase-3(C163S,V266H) and the wild type. We note that the observations made here can be only qualitative because thermodynamic parameters, such as *m*-values and ΔG°, can be established only in systems that are reversible.[21,29]

Equilibrium Folding of Procaspase-3(C163S,V266H) at pH 5. We next performed equilibrium unfolding and refolding measurements of procaspase-3(C163S,V266H) at pH 5 to determine the effect of changing the charge state of the histidine on the overall folding mechanism (Figure 3A). We observed that the samples that were equilibrated at low urea concentrations (0.25−2.75 M) precipitated during the incubation process, so these data points were omitted from further analysis. The unfolding data from fluorescence emission measurements, at all protein concentrations, show little to no change in signal from ∼3 to ∼4 M urea, followed by a cooperative decrease in the magnitude of the signal from ∼4 to ∼6 M urea. The CD data at 228 nm (■) show that the protein is largely unfolded from 6 to 9 M urea. The fluorescence emission data follow an apparent two-state equilibrium folding model, and the transition region displays a degree of cooperativity higher than that observed at pH 7. The $\text{urea}_{1/2}$ value for the transition is ∼5 M (fluorescence emission) and is estimated to be ∼3 M when measured by CD. Therefore, the tertiary structure appears to remain intact over a wider range of urea concentrations than the secondary structure, which is the opposite of the trends observed at pH 7.

The unfolding and refolding data are reversible at >3 M urea when they are measured by CD, at all protein concentrations examined (representative data shown in Figure 3B). The folding data measured by fluorescence emission demonstrate reversibility when the protein concentration is 2 μM, but data from lower protein concentrations are not reversible because of precipitation in the samples. For example, the signal for refolding is much weaker than that for unfolding, reaching ∼15 and ∼35% of the maximal signal given by the native dimeric protein for 0.5 and 1 μM protein, respectively (Figure 3C). When examined by SEC, the data show that, at pH 5, procaspase-3(C163S,V266H) is dimeric from 0 to 2 M urea, monomeric from 3 to 5 M urea, a

dx.doi.org/10.1021/bi400115n | *Biochemistry* 2013, 52, 3415−3427

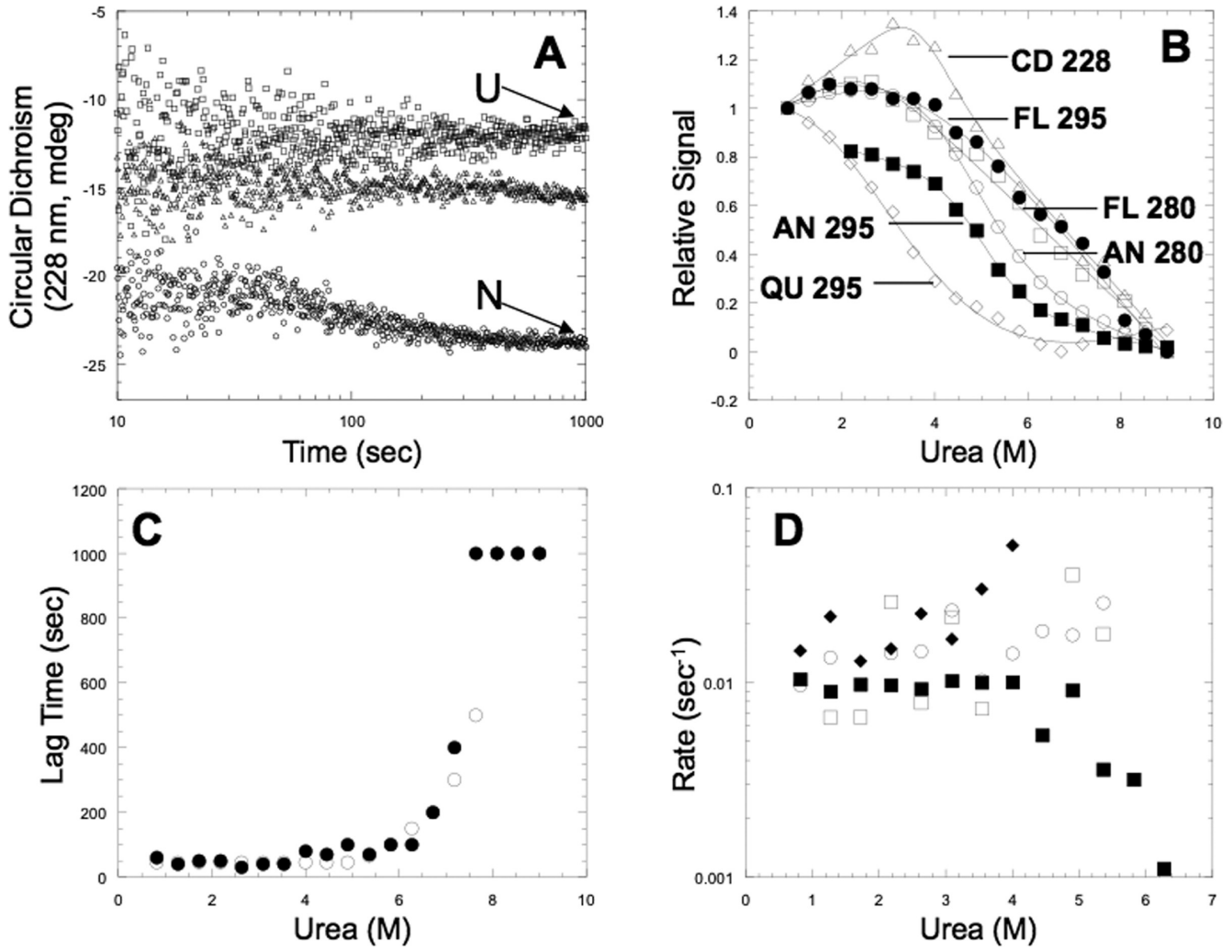

Figure 4. Refolding from urea. (A) First 1000 s of refolding as measured by CD at 228 nm. The unfolded (□) and native (○) protein signals as well as an intermediate urea concentration [4.45 M (△)] reveal four phases: burst, lag, intermediate, and slow. (B) Complex burst phase during refolding. The burst phase signal is plotted vs the final urea concentration for each detection method: differential quenching by acrylamide (◇), fluorescence emission at 340 nm with excitation at either 280 (□) or 295 nm (●), far-UV CD measured at 228 nm (△), and fluorescence anisotropy with excitation at either 280 (○) or 295 nm (■). The error bars represent the average from at least two experiments. The ΔG^{H_2O} values for the folding transition from fluorescence anisotropy experiments and differential quenching are 3.6 kcal/mol (excitation at 280 nm), 5.4 kcal/mol (excitation at 295 nm), and 1.0 kcal/mol, respectively. (C) Lag phase vs final urea concentration for 2 (●) and 10 μM protein (○) that shows that the length of the phase does not change with protein concentration. (D) Intermediate phase of refolding. Apparent rates of 100 s of refolding as detected by fluorescence with excitation at either 280 (○) or 295 nm (□), by differential quenching by acrylamide with excitation at 295 nm (◆), and by CD measured at 228 nm (■).

mixture of monomeric and unfolded protein in 6 M urea, and largely unfolded at 8 M urea, with a small fraction (<10%) of folded monomer. The intensity of the samples in 1 and 2 M urea-containing buffers is much lower because of the precipitation that occurs during sample incubation (Figure 3E), but on the basis of the elution profile of the native protein [Figure 3D (○)], the protein remaining in solution is dimeric. The presence of a stable monomeric species at pH 5 at intermediate urea concentrations differs from the SEC profile at pH 7, where the monomer is not observed as a separate species. The data from Figure 3D suggest that the monomeric species is larger than the unfolded state, but at present, it is unclear why it is in an expanded state relative to the unfolded monomer. We speculate that the peak represents an expanded monomer rather than a soluble aggregate species because of the lack of protein concentration dependence in the transition of the unfolding curve (Figure 3F). Taken together, with the unfolding data, the SEC peak that elutes at 8 mL is consistent with an expanded monomeric species. Therefore, the highly cooperative unfolding transition observed in equilibrium studies at pH 5 represents the unfolding of the monomer. This is shown schematically in Figure 3F.

Clearly, the introduction of a histidine into the dimer interface of procaspase-3 has a significant impact on the equilibrium folding mechanism, regardless of the pH, but the impact of the mutation cannot be fully understood because of the non-reversible folding pathways. The lack of reversibility and the absence of stable intermediates at equilibrium, as observed for wild-type procaspase-3 (Figure 1C,D), suggest that the system is under kinetic control.

Refolding Kinetics of Procaspase-3(C163S,V266H). We performed single-mixing refolding and unfolding studies using a variety of techniques to determine the differences in the folding mechanism of procapase-3(C163S,V266H) compared to that of the wild type. The kinetic folding mechanism of the wild type has been examined previously,[19] so the same studies were used in the

dx.doi.org/10.1021/bi400115n | *Biochemistry* 2013, 52, 3415−3427

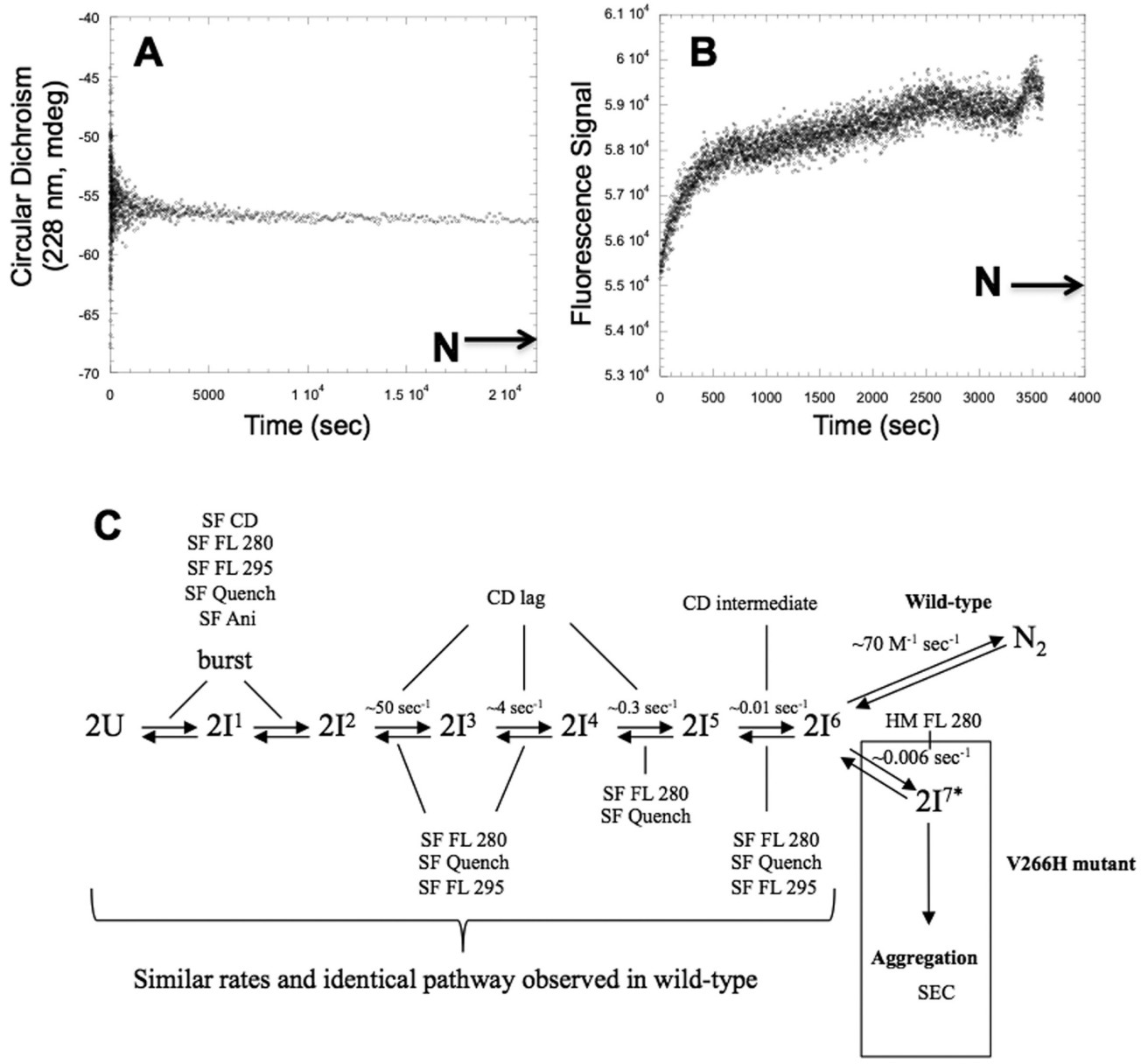

Figure 5. Slow phase of refolding that shows procaspase-3(C163S,V266H) enters a kinetic trap. The CD, measured at 228 nm (A), and differential quenching by acrylamide (B) signals were collected for 6 h on a steady state instrument. The native protein signal is marked (N). (C) Proposed sequential refolding mechanism. The unfolded protein folds though a series of monomeric intermediates (I^1–I^6) and becomes trapped in a conformation that is prone to aggregation (I^{7*}). The apparent rate of formation of each species is listed above each arrow. The detection methods are listed with the following abbreviations: SF, stopped-flow; CD, circular dichroism measured at 228 nm; FL, fluorescence with excitation at either 280 or 295 nm; quench, differential quenching by acrylamide with excitation at 295 nm; Ani, anisotropy with excitation at 280 and 295 nm; HM, hand-mixing studies; SEC, size exclusion chromatography.

characterization of the V266H variant to establish a direct comparison.

We examined the first 1000 s of refolding by monitoring the far-UV CD signal at 228 nm (Figure 4A). The data display four trends, which we refer to as burst, lag, intermediate, and slow. Identical trends were observed with similar kinetic rates during the refolding of the wild type, suggesting that the mutation does not affect the formation of secondary structure in this time frame.[19] We then used multiple detection methods to examine each of the regions in the refolding data (burst, lag, intermediate, and slow) to determine the effect of the mutation on the tertiary structure during folding. The experiments revealed the formation of multiple monomeric species in the burst phase followed by additional monomeric intermediates in the slower phases, which is again consistent with the folding of the wild type. The details of each of the four phases are discussed below.

The burst phase amplitudes from several detection methods are plotted as a function of urea concentration (Figure 4B) and reveal trends similar to those observed in the wild-type protein. All detection methods display a cooperative folding transition, indicating that the species formed in the burst phase correspond to structural changes in the protein. The data are not dependent on protein concentration, indicating that dimerization does not occur in the burst phase so the species formed are monomeric. A two-state folding model best describes each burst phase signal, although the data show that multiple species are formed because

dx.doi.org/10.1021/bi400115n | *Biochemistry* 2013, 52, 3415−3427

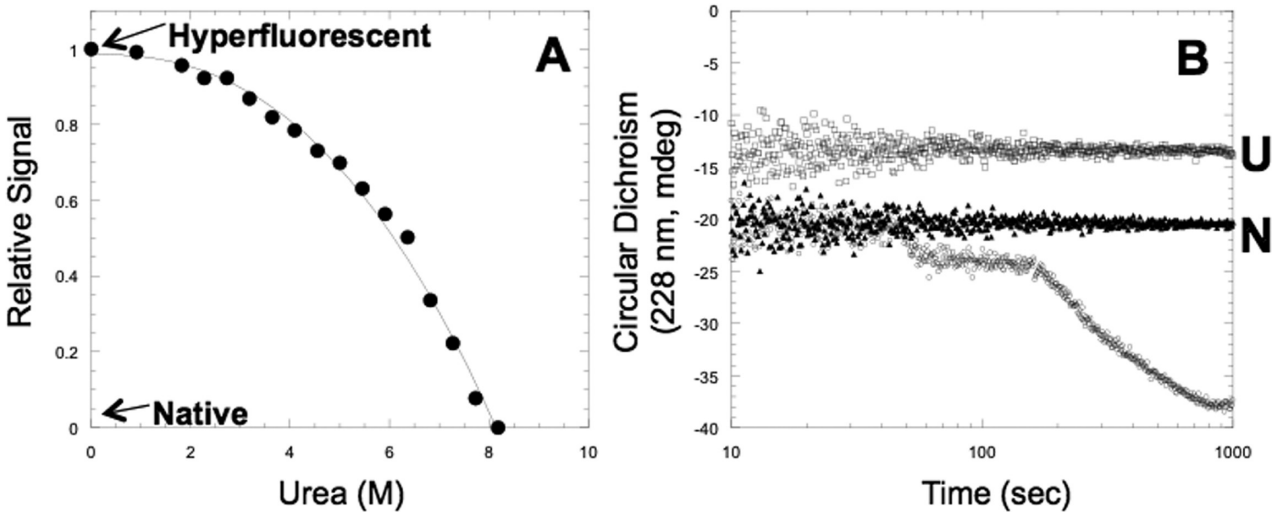

Figure 6. Unfolding kinetics. (A) Burst phase signal vs urea concentration measured by fluorescence emission. The line through the data was added for the sake of clarity and does not represent a fit. (B) First 1000 s of unfolding. Native procaspase-3(C163S,V266H) (110 μM) was mixed at a 1:10 ratio with 9 M urea-containing phosphate buffer (○). The native (▲) and unfolded (□) signals are shown.

the curves from multiple detection methods are noncoincident. We note one difference in the burst phase for the V266H variant compared to that of the wild type. For the mutant, at intermediate urea concentrations (3−4.5 M), the magnitude of the CD signal was ∼30% greater than the magnitude of the signal at lower urea concentrations. This suggests that, in the burst phase, the secondary structural content increases significantly at the intermediate urea concentrations and then decreases at lower urea concentrations. The ΔG^{H_2O} values for fluorescence anisotropy have an average of ∼4.5 kcal/mol. The stability of the burst phase species agrees well with that determined for the wild type (∼4.3 kcal/mol), although we note that the ΔG^{H_2O} value obtained for differential quenching is much lower than those from the other methods because the data have no pretransition.[30] Overall, the data suggest that the interface mutation does not affect formation of the burst phase species.

The burst phase was followed by multiple phases that also were not dependent on the protein concentration, demonstrating that these phases are associated with conformational changes in the monomer. For example, the far-UV CD data displayed a lag phase in the first ∼100 s of refolding, indicating that no changes to the secondary structure occurred in this time frame. The length of the lag increased with increasing concentrations of urea and was independent of protein concentration (Figure 4C), indicating that the lag phase is not due to dimerization. Overall, the data for the lag phase agree well with those determined previously for the wild-type protein.[19]

To monitor changes in tertiary structure during early refolding times, we examined the first 10 s of refolding by fluorescence emission (excitation at 280 or 295 nm) as well as differential quenching by acrylamide. The data for fluorescence emission (excitation at 280 nm) and differential quenching were best fit to a three-exponential equation, while fluorescence emission (excitation at 295 nm) data were best fit to a two-exponential equation. The amplitudes of the three phases were very small, suggesting that only minor structural changes were associated with these transitions. The apparent rates for the three phases are ∼50, ∼4, and ∼0.3 s^{-1} (data not shown). These data are very similar to those obtained previously for the refolding of the wild type using the same detection methods (∼50, ∼3, and 0.2 s^{-1}, respectively).[19] We previously interpreted the results as representing changes in minor populations of off-pathway species, and it appears the same species are present in the V266H variant. Together, the data indicate that the V266 to His mutation in the dimer interface does not alter the refolding mechanism in the first 10 s.

The next phase in the first 1000 s of refolding is termed the intermediate phase, when measured by far-UV CD. The apparent rate of this phase is 0.01 s^{-1} at lower urea concentrations, and the rate decreases with increasing concentrations of urea [Figure 4D (■)]. Fluorescence emission data were collected for the first 100 s of refolding and are best fit to a two-exponential equation. The first phase in this data set corresponds to the third phase in the 10 s data set, described above, indicating that the two experiments are monitoring the same structural change. The second phase corresponds to the "intermediate" phase described above for far-UV CD measurements. For all spectroscopic techniques, the apparent rates for the intermediate phase versus final urea concentration are shown in Figure 4D. The data show a limiting value of ∼0.01 s^{-1} at low urea concentrations regardless of technique. The rates gradually increase at higher urea concentrations, except when measured by CD, which decreases at higher urea concentrations as explained above. Very similar results were observed in the refolding of wild-type procaspase-3, where the intermediate phase is a complex process of multiple rates. Therefore, the V266H mutation does not affect the folding of the monomer in the first 100 s.

The final phase of refolding, as measured by far-UV CD, is the slow phase (Figure 5A). Refolding was monitored for 6 h (21600 s), and only a slight change in signal was observed. The data were fit to a single-exponential equation, with an apparent rate of 2.6×10^{-4} s^{-1} (data not shown). In contrast, the slow phase of refolding for the wild type has a half-time of ∼25 min.[19] These results suggest that the refolding pathway of the V266H variant diverges from that of the wild type during the slow phase of refolding. To examine this further, we performed hand-mixing refolding experiments and monitored changes in the differential quenching by acrylamide, which reports on the tryptophan residues in the active site. When similar studies were performed on the wild type, two phases were observed, neither of which was dependent on the protein concentration. In the first phase, the magnitude of the fluorescence signal increased, with a half-time

dx.doi.org/10.1021/bi400115n | *Biochemistry* 2013, 52, 3415−3427

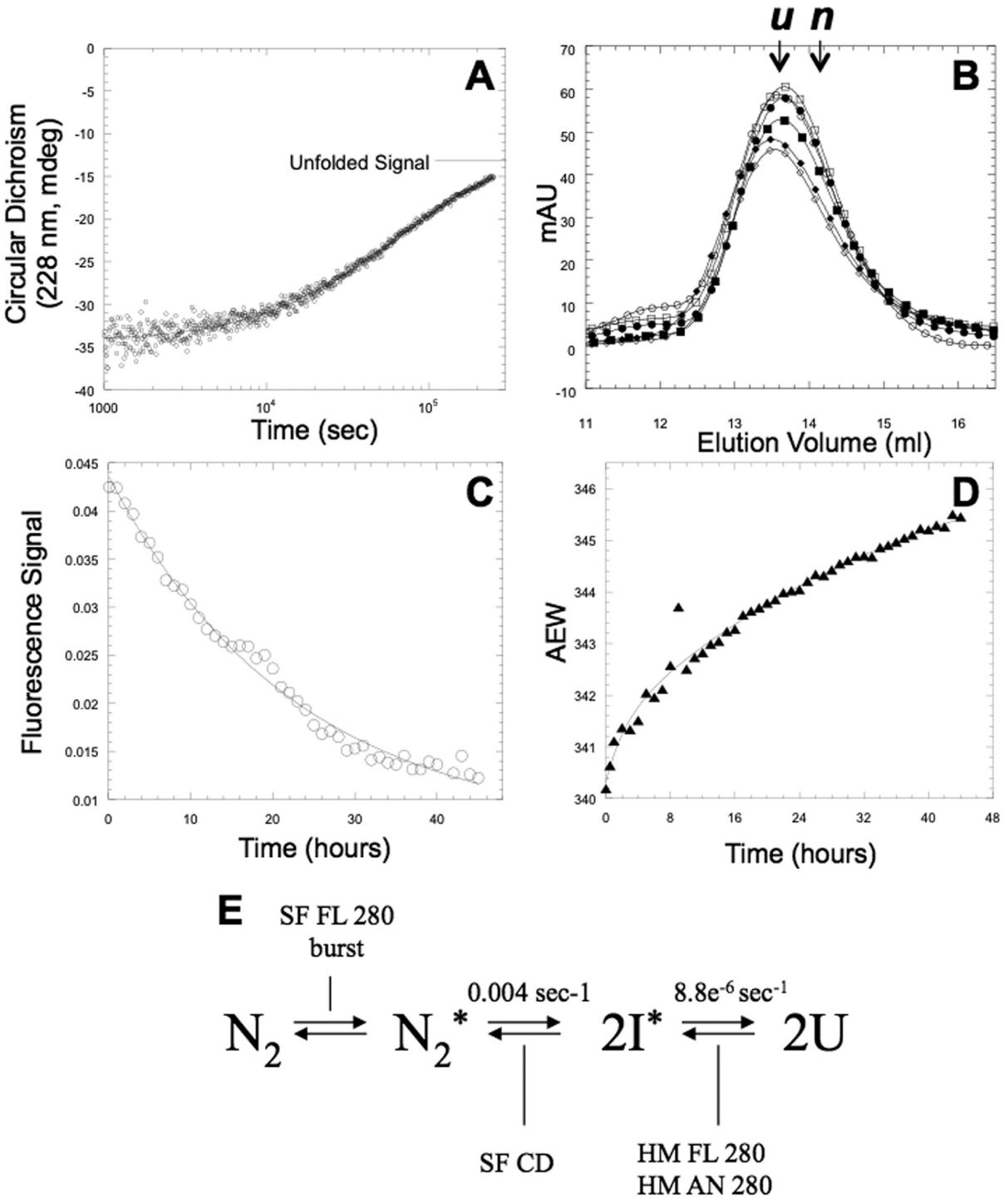

Figure 7. Slow phase of unfolding. (A) Far-UV CD signal measured at 228 nm after the sample had been unfolded for 72 h (○). The unfolded signal is marked. (B) Oligomeric state during the slow phase of unfolding. Native protein was manually mixed with 8 M urea and injected into the column after 1000 s (○), 4 h (●), 8 h (□), 25 h (■), 50 h (◇), and 72 h (◆) to monitor the oligomeric state of procaspase-3(C163S,V266H). The unfolded signal (u) and native signal (n) are marked. (C and D) Signals of fluorescence anisotropy with excitation at 280 nm (C) and fluorescence emission at 340 nm with excitation at 280 nm (D) were collected every hour for 45 h on a steady state instrument. Fluorescence emission data (D) are plotted as the average emission wavelength. (E) Proposed sequential unfolding mechanism. The native dimer forms a hyperfluorescent species in the burst phase (N_2*) that dissociates to form an ultrastable monomeric intermediate (2I*) that slowly unfolds. The apparent rate of formation of each species is shown. The detection methods are listed with the following abbreviations: SF, stopped-flow; CD, circular dichroism measured at 228 nm; FL, fluorescence with excitation at 280 nm; An, anisotropy with excitation at 280 nm; HM, hand-mixing studies.

of ~8 min, indicating the tryptophan residues entered a more hydrophobic environment. The magnitude of the fluorescence signal decreased during the second phase, with a half-time of ~25 min, indicating the exposure of the active site to solvent. Similar studies of the V266H variant also revealed two phases (Figure 5B). During the first phase, the magnitude of the fluorescence signal increased, with a half-time of ~7 min, which is consistent with the data for the wild type and indicates that the tryptophan

dx.doi.org/10.1021/bi400115n | *Biochemistry* 2013, 52, 3415−3427

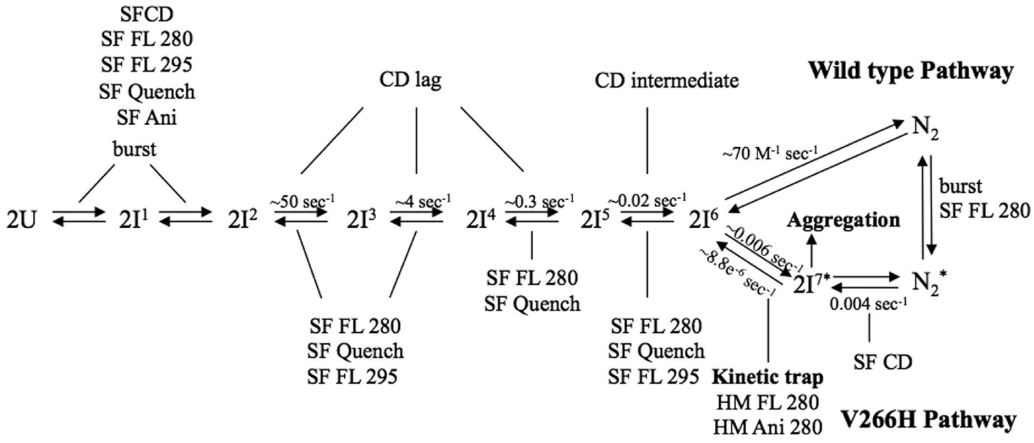

Figure 8. Proposed overall folding mechanism for procapase-3(C163S,V266H). Figures 5C and 7E were merged to give the proposed overall folding mechanism of procaspase-3(C163S,V266H). Abbreviations on this figure were previously defined.

residues in the active site enter a more hydrophobic environment. In the second phase, however, the magnitude of the fluorescence signal continued to increase, in contrast to the data for the wild type. Thus, for the V266H variant, the signal did not reach that of the native protein on the time scale of these experiments. Because the refolding of the V266H variant was very slow, we used SEC and native polyacrylamide gel electrophoresis to determine the oligomeric state of the protein throughout the time frame used in the hand-mixing experiments. The results showed that the protein remained a monomer and aggregated slowly, rather than forming a dimer (data not shown).

The simplest kinetic folding model to describe the single-mixing refolding data is shown in Figure 5C. We recognize that some of the intermediates described above could be off-pathway or in parallel folding pathways. At this point, our data do not address these issues, so we prefer to use the simplest scheme when comparing the results to those of the wild type. In this sequential folding mechanism, the protein forms multiple monomeric species in the burst phase followed by a series of monomeric intermediates. The intermediates are simply described by the apparent rates of formation and the techniques used to monitor those rates. At longer times, the protein folds into a species (I^6 in Figure 5D) that either forms a dimer (N_2) or becomes kinetically trapped and is prone to aggregation (I^7*). The rates for each phase as well as their respective detection method(s) can be found in Figure 5D.

Unfolding Kinetics of Procaspase-3(C163S,V266H). Single-mixing unfolding studies were performed using fluorescence emission (excitation at 280 nm), and the data reveal a single burst phase (data not shown). A plot of the burst phase amplitude versus final urea concentration displayed a cooperative transition in which a hyperfluorescent species was formed after the sample had been mixed for 1−2 ms (Figure 6A). We could not fit the data to an equilibrium folding model due to the absence of a post-transition region, but the results indicate the presence of a dimeric ensemble that differs from the native protein. Similar studies of the wild type revealed a similar burst phase and the presence of a hyperfluorescent species. A single-mixing unfolding study in which the far-UV CD was monitored for 1000 s was performed [Figure 6B (○)]. When the protein is rapidly mixed with 8 M urea, the magnitude of the signal increases (becomes more negative) by 2-fold compared to the native control (triangles), indicating the formation of an ultrastructured species. The native protein converts to this species through two transitions. Initially, a lag phase was observed in the first ∼50 s of unfolding, where the signal remained constant. Following the lag phase, one observes a small increase in the magnitude of the signal. The second transition occurred between ∼150 and 1000 s of unfolding and resulted in a large increase in the magnitude of the signal, demonstrating a large increase in secondary structural content. Approximately 70% of the overall change in the signal occurred in the second transition, with an apparent rate of 0.004 s^{-1}. We used SEC to determine the oligomeric state of the protein after it had been unfolded for 1000 s (see Figure 7B), and the results show that the protein is monomeric.

Hand-mixing far-UV CD experiments were performed for 72 h to determine the rate of unfolding for the ultrastructured monomeric intermediate (Figure 7A). The data show that the intermediate unfolds with a half-time of ∼18 h (apparent rate for the transition of 1.7×10^{-5} s^{-1}). We then used SEC to determine the oligomeric state of the protein throughout this time frame (Figure 7B), and the resulting chromatograms show that the protein is a monomer at all of the time points. We also performed hand-mixing unfolding experiments for 45 h using both fluorescence spectroscopy and fluorescence anisotropy (excitation at 280 nm) to determine the tertiary structural changes that occur during unfolding of the monomer (Figure 7C,D). The results show a decrease in anisotropy with a half-time of ∼16 h for the transition (Figure 7C) (apparent rate of 1.2×10^{-5} s^{-1}). The results for fluorescence spectroscopy reveal a single cooperative transition with a half-time of ∼16 h (apparent rate of 7.7×10^{-6} s^{-1}) (data not shown). The fluorescence emission data were also plotted as the average emission wavelength versus time (Figure 7D), and the data show a cooperative transition that is best described by a two-exponential equation. The apparent rate for the slower phase is 6.7×10^{-6} s^{-1}, which agrees well with the apparent rate observed by the single-wavelength analysis (340 nm) and anisotropy. The fluorescence emission becomes red-shifted over time, indicating that the aromatic residues become more solvent-exposed.

Overall, the results from the unfolding experiments show that the ultrastructured monomeric intermediate unfolds very slowly, where the half-times of unfolding are similar in all detection methods and are in the range of 16−18 h. The apparent rates for unfolding of the tertiary structure have an average of 8.8×10^{-6} s^{-1}, and the apparent rate for unfolding of the secondary structure is 1.7×10^{-5} s^{-1}. The simplest kinetic unfolding model

dx.doi.org/10.1021/bi400115n | *Biochemistry* 2013, 52, 3415−3427

to describe the single-mixing unfolding data is shown in Figure 7E. In this sequential folding mechanism, the native dimer (N_2) forms a hyperfluorescent dimeric species in the burst phase (N_2*). The dimer dissociates after ~50 s and forms an ultrastructured monomeric intermediate (2I*), which slowly unfolds (2U). The apparent rates for each phase as well as their respective detection method(s) are shown in Figure 7E.

A comprehensive folding model, combining the refolding and unfolding reactions for procaspase-3(C163S,V266H) and the wild type, is shown in Figure 8. We again recognize that the data presented here do not rule out more complicated off-pathway or parallel models, but we provide the schematic simply as a framework to compare the two proteins and the results of the interface mutations.

DISCUSSION

The equilibrium and kinetic folding studies of procaspase-3(C163S,V266H) revealed that the interface mutation has a significant impact on dimer assembly. A hysteresis in the equilibrium unfolding and refolding studies at pH 7 shows that the reactions do not reach equilibrium within 24 h. The hysteresis is dependent on the protein concentration as shown by a closer agreement in signal between the refolding and unfolding data as the concentration of protein increased. We could not determine the dimerization step during equilibrium folding at pH 7 because of the absence of a protein concentration-dependent transition. Instead, we observed a broad cooperative transition over a large range of urea concentrations, and data from SEC showed that both monomeric and dimeric species are populated at the intermediate urea concentrations. It is not clear whether the intermediates [I_2 and I (Figure 1C)] observed for the wild-type protein are present during the equilibrium unfolding of the V266H variant at pH 7.

Equilibrium studies of procaspase-3(C163S,V266H) at pH 5 reveal that the protein precipitates at low urea concentrations (<3 M). At >3 M urea, the protein unfolds cooperatively and reversibly by an apparent two-state equilibrium folding model. On the basis of SEC elution profiles, this transition represents the unfolding and refolding of the monomer, whereas the dimer is present at lower urea concentrations. The data at pH 5 indicate that the histidine in the interface destabilizes the dimer such that it is more prone to aggregation, although at present the mechanism for this process it is not known. Clearly, the introduction of a histidine into the dimer interface of procaspase-3 has a significant impact on the equilibrium folding mechanism, regardless of pH.

Because the equilibrium data demonstrated that the folding is under kinetic control, we performed kinetic refolding and unfolding studies using a variety of spectroscopic probes to determine the effect of the mutation on the overall folding mechanism. Refolding studies demonstrated that the monomer of the V266H variant refolds like that of the wild type within the first 100 s of refolding. At longer times, however, the pathways diverge. In the case of the wild-type protein, the monomer dimerizes slowly (~70 M^{-1} s^{-1}) following the formation of a dimerization competent intermediate. In the case of procaspase-3(C163S,V266H), we were unable to monitor an association step for the monomer at the longer refolding times. The results indicate that the histidine side chains in the interface decrease the rate of dimerization, which is already quite slow in the wild-type protein. As a result, the monomer forms a species that becomes kinetically trapped and is prone to aggregation. Recent structural studies of cleaved caspase-3(V266H), and variants thereof,[15] show that the histidine side chains pack in a face-to-face manner because of steric hindrance in the interface (Figure 1B). The packing of the histidine residues causes significant movements in several amino acids, starting at Y197 in the dimer interface, which propagates to the active site, causing movement of the catalytic histidine, H121. These events cause occlusion of the S1 substrate-binding pocket and a disordering of the active site loop, L1. When the adjacent Y197 is mutated to a smaller side chain (Y197C) in the presence of H266, the histidines are observed in the more favored rotamer that places the side chains edge-on (Figure 1B). By extension to the procaspase, we presume that the histidine side chain is in the more preferred rotamer during folding of the monomer but must change to the less preferred rotamer to dimerize. As a result, an inefficient encounter complex, as previously described for wild-type procaspase-3, is even less efficient in the V266H variant. During refolding, therefore, a kinetic competition between formation of the correct rotamer to allow dimerization and aggregation of the monomer occurs. This interpretation is consistent with our observation of an increased level of aggregation at lower protein concentrations and a closer agreement of the folding−unfolding transitions in the equilibrium data at higher protein concentrations.

As noted above, the rate of dimerization for wild-type procaspase-3 is ~70 M^{-1} s^{-1}, which is slow compared to those of other homodimers. For example, bacterial luciferase has a rate of dimerization of 2.4×10^3 M^{-1} s^{-1} and the P_{22} arc repressor has a dimerization rate of ~10^7 M^{-1} s^{-1}.[31,32] We note, however, the rate of dimerization of procaspase-3 is significantly higher than that of procaspase-8, an initiator procaspase. In that case, procaspase-8 requires oligomeric activating complexes to promote dimerization *in vivo*. Because of the so-called "induced proximity" effect, the death complex sufficiently increases the local protein concentration to induce dimerization.[3,7] Procaspase-8 also has been shown to form dimers *in vitro* in the presence of kosmotropes, such as sodium citrate.[3,6] The rate of procaspase-8 dimerization in the presence of a high salt concentration (1 M sodium citrate) was shown to be ~5×10^3 M^{-1} s^{-1}.[6] Extrapolation of the apparent rate obtained at several salt concentrations to the absence of salt reveals a second-order rate of approximately zero. The procaspase-8 dimer interface contains "negative design" elements in that F468 from one monomer stacks on P466′ of the second monomer (the prime indicates the amino acid resides in the second monomer). Likewise, F468′ interacts with P466. Other initiator procaspases also have bulky aromatic residues in their dimer interfaces that result in intersubunit stacking interactions upon dimerization.[5,33] The requirement of the optimal side chain−side chain interactions, rather than just backbone hydrogen bonds, presumably prevents indiscriminate association of the exposed β-strand 8. At present, it is not clear how these elements affect the rate of dimerization, but it is well-known that dimerization of initiator procaspases is a key regulatory mechanism of apoptosis.[4,34] We suggest that the presence of the histidine in the dimer interface of procaspase-3 introduces a negative design element by requiring a rotamer with a low population to alleviate steric clashes upon dimerization. The presence of H266 in procaspase-3 effectively changes the assembly of an effector caspase to mimic that of an initiator caspase, as the rates of dimerization for initiators and of the V266H variant are very low in the absence of other factors. Overall, the data presented here suggest that the introduction of a negative design element in the dimer interface may provide a checkpoint in apoptosis so that it is

dx.doi.org/10.1021/bi400115n | *Biochemistry* 2013, 52, 3415−3427

not prematurely initiated in the absence of a death signal. This may be an important consideration in the evolution of the caspase proteins because the current family of human caspases evolved from a monomeric progenote.[35,36] The data presented here suggest that the dimeric effector procaspases could evolve from the monomeric ancestral protein via improvement by nature of the encounter complex of the monomer such that the rate of dimerization is increased.

AUTHOR INFORMATION

Corresponding Author

*Department of Molecular and Structural Biochemistry, 128 Polk Hall, North Carolina State University, Raleigh, NC 27695-7622. E-mail: clay_clark@ncsu.edu. Phone: (919) 515-5805. Fax: (919) 515-2047.

Funding

This work was supported by National Institutes of Health Grant GM065970 to A.C.C.

Notes

The authors declare no competing financial interest.

ACKNOWLEDGMENTS

We thank the research agencies of North Carolina State University and the North Carolina Agricultural Research Service.

ABBREVIATIONS

IL, intersubunit linker; SEC, size exclusion chromatography; CD, circular dichroism; wild type, procaspase-3(C163S); PDB, Protein Data Bank.

REFERENCES

(1) Fuentes-Prior, P., and Salvesen, G. S. (2004) The protein structures that shape caspase activity, specificity activation and inhibition. *Biochem. J. 384*, 201−232.

(2) MacKenzie, S. H., and Clark, A. C. (2008) Targeting cell death in tumors by activating caspases. *Curr. Cancer Drug Targets 8*, 98−109.

(3) Boatright, K. M., Renatus, M., Scott, F. L., Sperandio, S., Shin, H., Pedersen, I. M., Ricci, J.-E., Edris, W. A., Sutherlin, D. P., Green, D. R., and Salvesen, G. (2003) A unified model for apical caspase activation. *Mol. Cell 11*, 529−541.

(4) Boatright, K. M., and Salvesen, G. S. (2003) Mechanisms of caspase activation. *Curr. Opin. Cell Biol. 15*, 725−731.

(5) Renatus, M., Stennicke, H. R., Scott, F. L., Liddington, R. C., and Salvesen, G. S. (2001) Dimer formation drives the activation of the cell death protease caspase 9. *Proc. Natl. Acad. Sci. U.S.A. 98*, 14250−14255.

(6) Pop, C., Fitzgerald, P., Green, D. R., and Salvesen, G. S. (2007) Role of proteolysis in caspase-8 activation and stabilization. *Biochemistry 46*, 4398−4407.

(7) Muzio, M., Stockwell, B. R., Stennicke, H., Salvesen, G. S., and Dixit, V. M. (1998) An induced proximity model for capase-8 activation. *J. Biol. Chem. 273*, 2926−2930.

(8) Pop, C., and Salvesen, G. S. (2009) Human Caspases: Activation, Specificity and Regulation. *J. Biol. Chem. 284*, 21777−21781.

(9) Van Raam, B. J., and Salvesen, G. S. (2012) Proliferative versus apoptotic functions of caspase-8. Hetero or homo: The caspase-8 dimer controls cell fate. *Biochim. Biophys. Acta 1824*, 113−122.

(10) Stennicke, H. R., and Salvesen, G. S. (1998) Properties of the caspases. *Biochim. Biophys. Acta 1387*, 17−31.

(11) Pop, C., Chen, Y.-R., Smith, B., Bose, K., Bobay, B., Tripathy, A., Franzen, S., and Clark, A. C. (2001) Removal of the pro-domain does not affect the conformation of the procaspase-3 dimer. *Biochemistry 40*, 14224−14235.

(12) Bose, K., Pop, C., Feeney, B., and Clark, A. C. (2003) An uncleavable procaspase-3 mutant has a lower catalytic efficiency but an active site similar to that of mature caspase-3. *Biochemistry 42*, 12298−12310.

(13) Richardson, J. S., and Richardson, D. C. (2002) Natural β-sheet proteins use negative design to avoid edge-to-edge aggregation. *Proc. Natl. Acad. Sci. U.S.A. 99*, 2754−2759.

(14) Pop, C., Feeney, B., Tripathy, A., and Clark, A. C. (2003) Mutations in the procaspase-3 dimer interface affect the activity of the zymogen. *Biochemistry 42*, 12311−12320.

(15) Walters, J. A., Schipper, J. L., Swartz, P., Mattos, C., and Clark, A. C. (2012) Allosteric modulation of caspase-3 through mutagenesis. *Biosci. Rep. 32*, 401−411.

(16) Hardy, J. A., Lam, J., Nguyen, J. T., O'Brien, T., and Wells, J. A. (2004) Discovery of an allosteric site in the caspases. *Proc. Natl. Acad. Sci. U.S.A. 101*, 12461−12466.

(17) Scheer, J. M., Romanowski, M. J., and Wells, J. A. (2006) A common allosteric site and mechanism in caspases. *Proc. Natl. Acad. Sci. U.S.A. 103*, 7595−7600.

(18) Bose, K., and Clark, A. C. (2001) Dimeric procaspase-3 unfolds via a four-state equilibrium process. *Biochemistry 40*, 14236−14242.

(19) Milam, S. L., and Clark, A. C. (2009) Folding and assembly kinetics of procaspase-3. *Protein Sci. 18*, 2500−2517.

(20) Walters, J. A., Milam, S. L., and Clark, A. C. (2009) Practical approaches to protein folding and assembly: Spectroscopic strategies in thermodynamics and kinetics. *Methods Enzymol. 455*, 1−39.

(21) Pace, C. N. (1986) Determination and analysis of urea and guanidine hydrochloride denaturation curves. *Methods Enzymol. 131*, 266−280.

(22) Ryser, S., Vial, E., Magnenat, E., Schlegel, W., and Maundrell, K. (1999) Reconstitution of caspase-mediated cell-death signalling in *Schizosaccharomyces pombe*. *Curr. Genet. 36*, 21−28.

(23) Fernandes-Alnemri, T., Litwack, G., and Alnemri, E. S. (1994) CPP32, a novel human apoptotic protein with homology to *Caenorhabditis elegans* cell death protein Ced-3 and mammalian interleukin-1-β converting enzyme. *J. Biol. Chem. 269*, 30761−30764.

(24) Dorstyn, L., Kinoshita, M., and Kumar, S. (1998) Caspases in cell death. *Results Probl. Cell Differ. 24*, 1−24.

(25) Stennicke, H. R., and Salvesen, G. S. (1999) Catalytic properties of the caspases. *Cell Death Differ. 6*, 1054−1059.

(26) Stennicke, H. R., and Salvesen, G. S. (1999) Caspases: Preparation and characterization. *Methods 17*, 313−319.

(27) Feeney, B., and Clark, A. C. (2005) Reassembly of active caspase-3 is facilitated by the propeptide. *J. Biol. Chem. 280*, 39772−39785.

(28) Milam, S. L., Nicely, N. I., Feeney, B., Mattos, C., and Clark, A. C. (2007) Rapid folding and unfolding of Apaf-1 CARD. *J. Mol. Biol. 369*, 290−304.

(29) Pace, C. N., Shirley, B. A., and Thomson, J. A. (1989) Measuring the conformational stability of a protein. In *Protein Structure and Function, A Practical Approach* (Creighton, T., Ed.) pp 311−329, IRL Press, New York.

(30) Santoro, M. M., and Bolen, D. W. (1988) Unfolding free energy changes determined by the linear extrapolation method. 1. Unfolding of phenylmethanesulfonyl α-chymotrypsin using different denaturants. *Biochemistry 27*, 8063−8068.

(31) Clark, A. C., Raso, S. W., Sinclair, J. F., Ziegler, M. M., Chaffotte, A. F., and Baldwin, T. O. (1997) Kinetic mechanism of luciferase subunit folding and assembly. *Biochemistry 36*, 1891−1899.

(32) Milla, M. E., and Sauer, R. T. (1994) P22 arc repressor: Folding kinetics of single-domain, dimeric protein. *Biochemistry 33*, 1125−1133.

(33) Watt, W., Koeplinger, K. A., Mildner, A. M., Heinrikson, R. L., Tomasselli, A. G., and Watenpaugh, K. D. (1999) The atomic-resolution structure of human capase-8, a key activator of apoptosis. *Structure 7*, 1135−1143.

(34) Wachmann, K., Pop, C., Van Raam, B. J., Drag, M., Mace, P. D., Snipas, S. J., Zmasek, C., Schwarzenbacher, R., Salvesen, G. S., and Riedl, S. J. (2010) Activation and specificity of human caspase-10. *Biochemistry 49*, 8307−8315.

(35) Wang, Y., and Gu, X. (2001) Functional divergence in the caspase gene family and altered functional constraints: Statistical analysis and prediction. *Genetics 158*, 1311−1320.

(36) Lamkanfi, M., Declercq, W., Kalai, M., Saelens, X., and Vandenabeele, P. (2002) Alice in caspase land. A phylogenetic analysis of caspases from worm to man. *Cell Death Differ. 9*, 358−361.